Supplement of Earth Syst. Sci. Data, 18, 6589–6611, 2026
https://doi.org/10.5194/essd-18-6589-2026-supplement

Supplement of

Global satellite gravity data products for prompt detection of short-term Mass Change (MC)

Miao Tang et al.

Correspondence to: Shin-Chan Han (han.104@osu.edu)

Figure S1

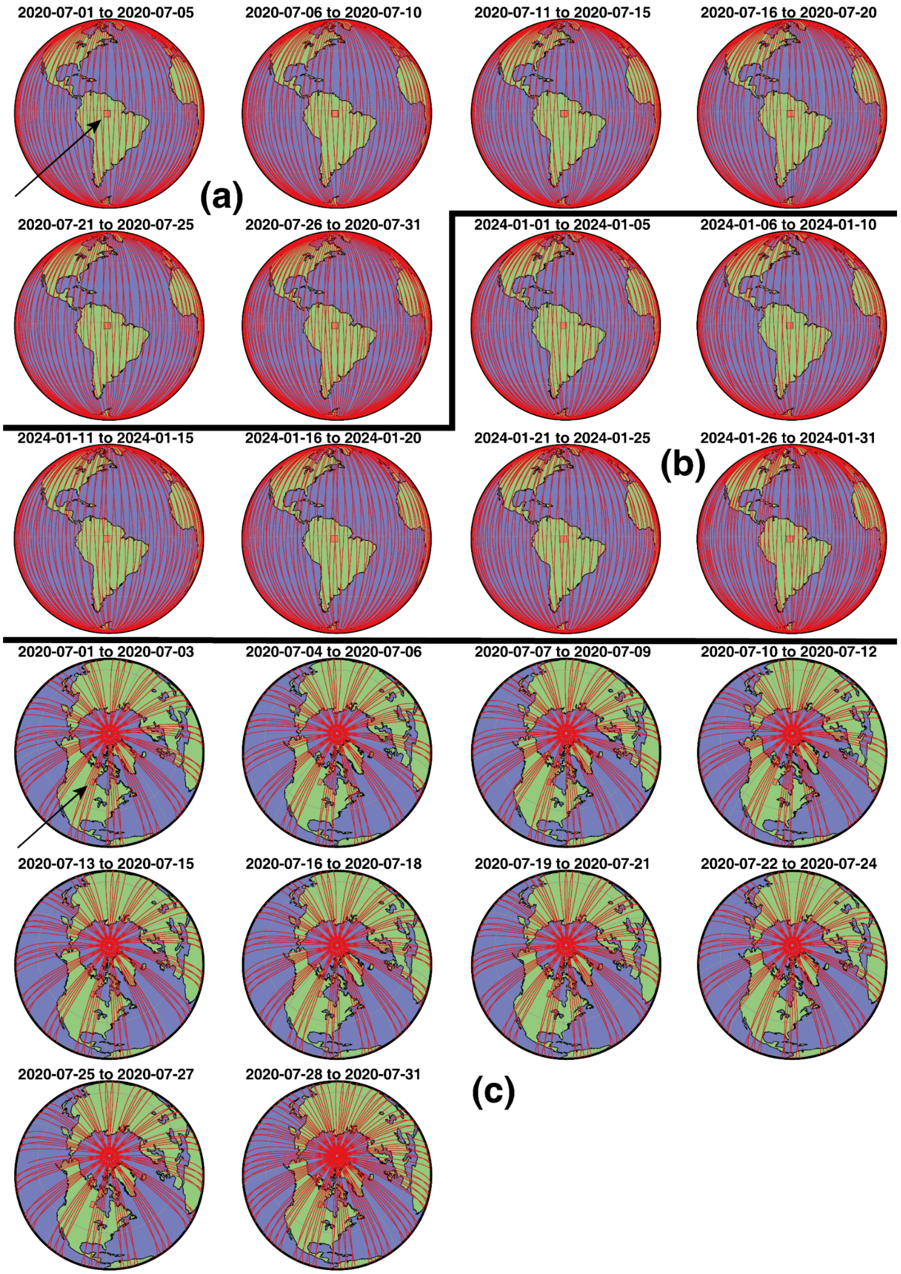

Figure S1. Satellite ground tracks (red curves) in consecutive 5-day windows during July 2020 for a low- to mid-latitude case (a), in consecutive 5-day windows during January 2024 for comparison (b), and in consecutive 3-day windows during July 2020 for a high-latitude case (c). The red 4°×4° boxes mark the study areas in the Amazon (a and b) and North America (c).

Figure S2

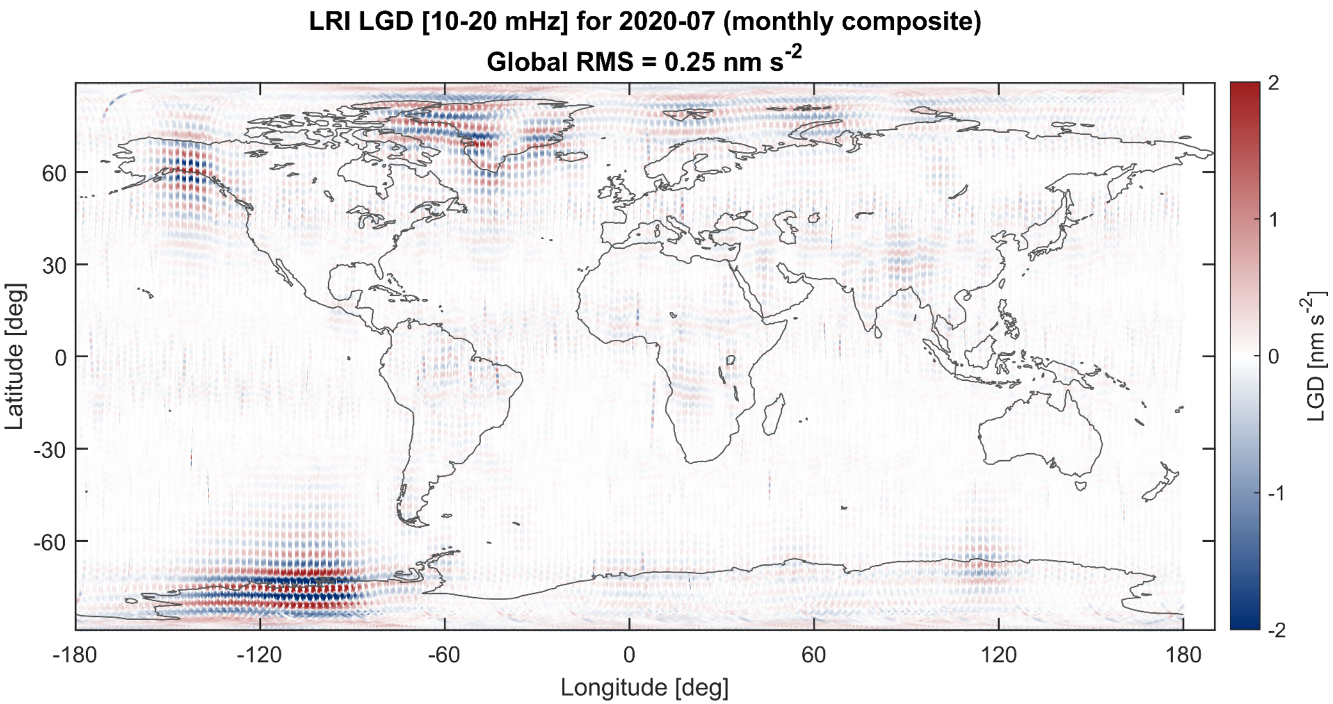

15 **Figure S2**. Global distribution of monthly composite LRI-LGD in the 10–20 mHz band for July 2020.

Figure S3

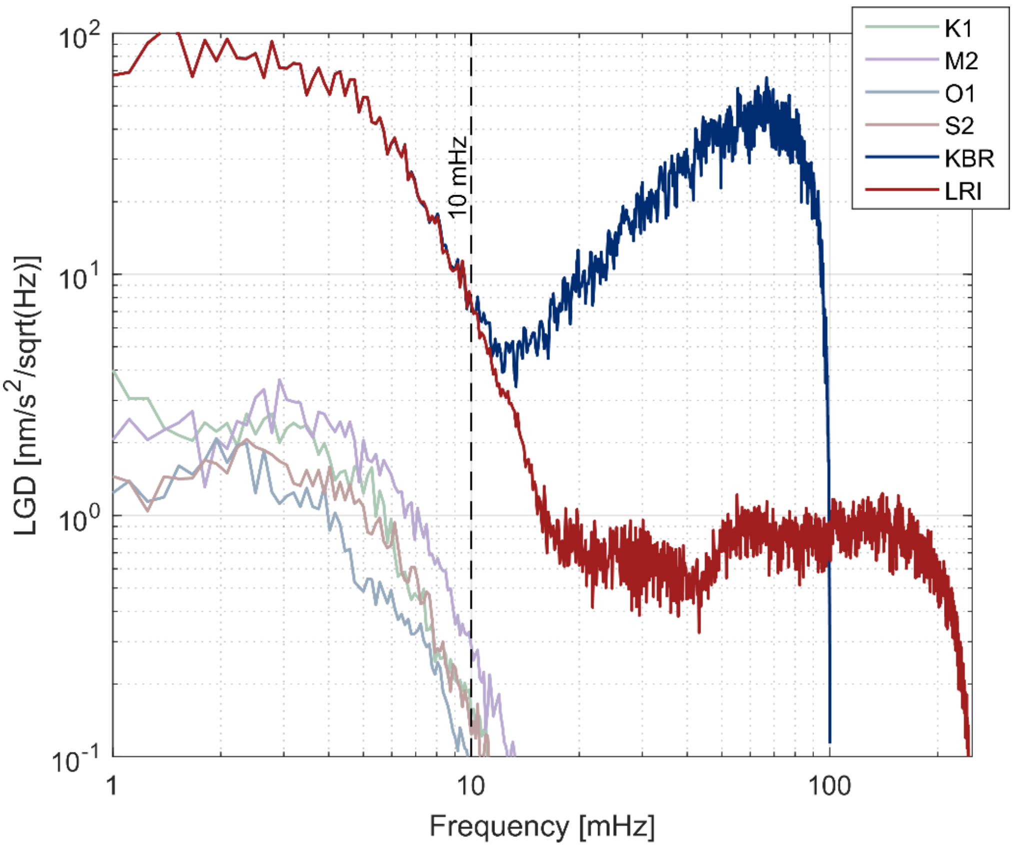

Figure S3. Amplitude spectral density of the LGD differences on 18 July 2020 resulting from two alternative ocean tide models (FES2014b and GOT4.7), shown for the main tidal constituents K1, M2, O1, and S2. The KBR-LGD and LRI-LGD spectra are also shown for comparison. The results show that the amplitudes of model differences remain much smaller than the LGD signal itself. In terms of RMS, the values are 0.14, 0.17, 0.08, and 0.10 nm/s^{-2} for K1, M2, O1, and S2, respectively.

Section S1

The LGD values in our final dataset are referenced only to the static part of GOCO06s, rather than to the static, annual, and trend components combined. Although the reference orbit determination uses all three components (i.e., the static, annual, and trend parts), the LGD contributions corresponding to the annual and trend signals are added back in the final processing step. Therefore, the released LGD dataset is effectively expressed with respect to the static gravity field only, so that the full time-varying gravity signal is preserved. The corresponding processing flow is illustrated in Fig. S4.

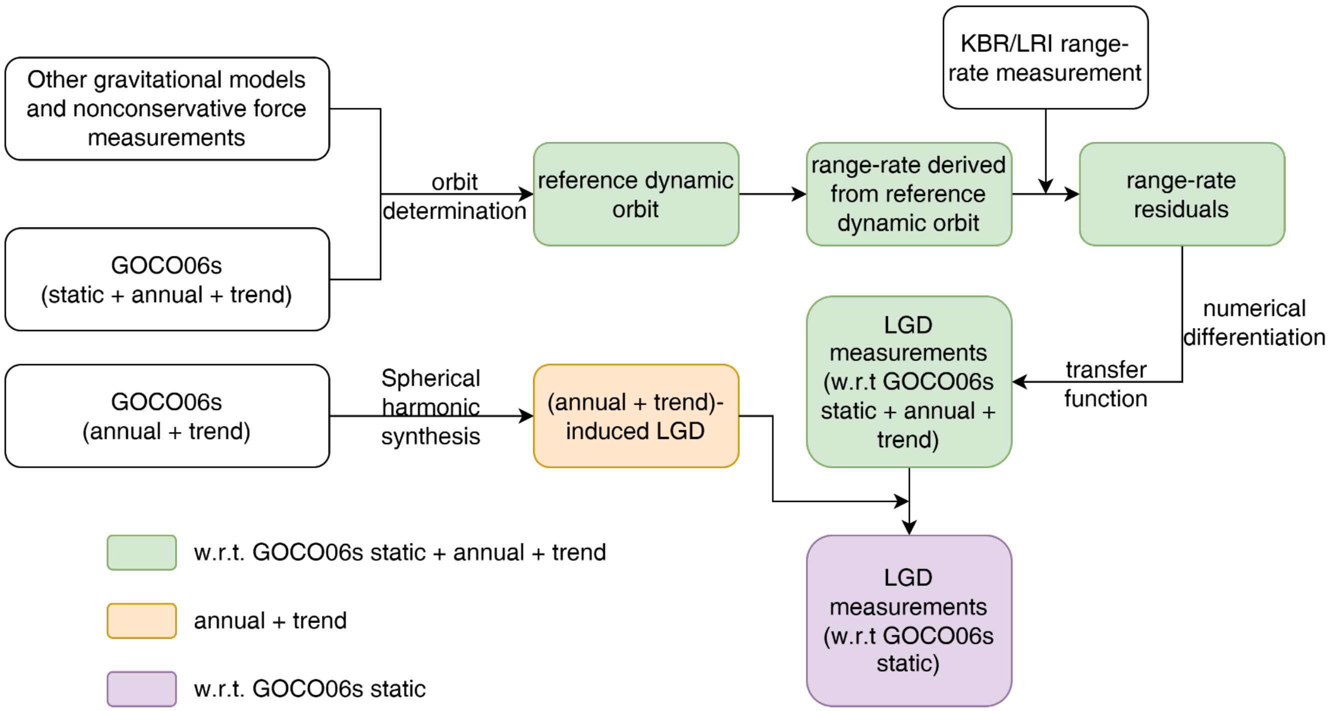

Figure S4. Processing flow for deriving the final LGD measurements with respect to the static part of GOCO06s.

Section S2

In this study, the climatology fit is estimated using GRACE CSR RL06 and GRACE-FO CSR RL06.3 gravity field solutions from 2002 to 2024. The processing strategy is as follows:

(1) We collect the spherical harmonic solutions, replace $C_{2,0}$ and $C_{3,0}$ with SLR-derived estimates, and remove the static field of GOCO06s.

(2) For each Stokes coefficient time series, we perform a least-squares fit consisting of a linear trend, a seasonal term, and residuals. Note that the least-squares adjustment used here is not a six-parameter model. Instead, each cosine and sine spherical harmonic coefficient is fitted separately using a 13-parameter model comprising one linear trend and 12 monthly climatological coefficients, one for each calendar month. No additional constant term is included because the 12 monthly indicator terms already represent the month-dependent intercepts. The model can be expressed as:

$$y(t_i) = \dot{y}(t_i - t_0) + \sum_{k=1}^{12} M_k(t_i)\beta_k + \varepsilon_i$$

where $\dot{y}$ denotes the linear trend, t_0 is the reference epoch of GOCO06s (i.e., 2010.0), $M_k(t_i)$ is a monthly indicator function, and β_k is the climatological coefficient for month k. An initial fit is performed, observations with residuals exceeding three standard deviations are identified as outliers, and the model is then refitted after excluding these observations.

(3) The climatological coefficients for each target date are obtained from the fitted model, and the climatological LGD is then synthesized from these coefficients.

Section S3

The LGD_full product retains the complete L1B-derived signal above 1 mHz and is supplemented with the L2-derived low-frequency component (<1 mHz), without applying any high-frequency filtering. In contrast, the LGD_band product is obtained by applying a band-pass filter to suppress high-frequency instrument noise (10–100 mHz for KBR-LGD and 20–250 mHz for LRI-LGD), while the same L2-derived low-frequency component (<1 mHz) is added to recover the full-spectrum gravity signal. Details of the frequency-domain processing are provided in Fig. S5.

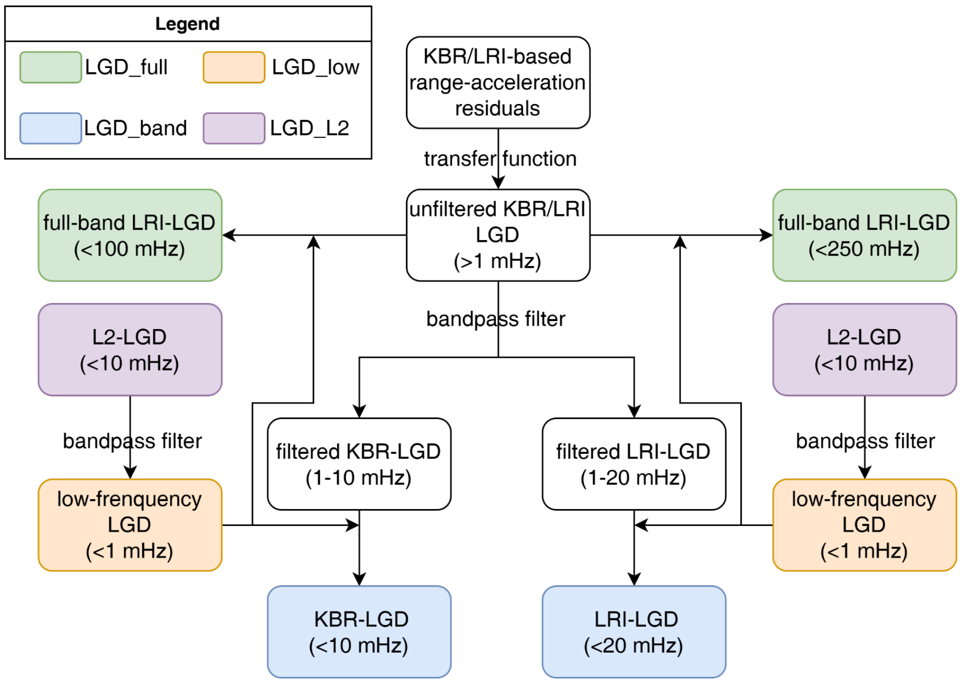

Figure S5. Schematic illustration of the frequency content of the LGD products derived from KBR/LRI observations and L2 solutions.

Section S4

When constructing a regional LGD time series, we need to integrate the along-track LGD measurement time series crossing the study area, which is done through a weighted average (as shown in Figs. S6a and S6b). Sensitivity analysis (Figs. S6c and S10d) shows that the maximum LGD response is contributed by surface mass directly beneath the satellite track, and the response decays rapidly with increasing distance from the load center. Therefore, when focusing on a specific study region, LGD observations near the boundary are more likely to be influenced by mass changes outside the target region and should not be integrated with equal weight. For this reason, we apply a Gaussian-based weighting when integrating the along-track LGD observations into a regional time series. The corresponding weighting formula is:

$$LGD_i = \frac{\sum_{j=1}^{N} w_j LGD_{i,j}}{\sum_{j=1}^{N} w_j}$$

where $LGD_{i,j}$ is the j-th along-track LGD measurement on date i. For a given date i, LGD_i represents the regional LGD (Figure S10b) derived from the LGD measurements crossing the target region. Here, N is the number of observations within the target region, and w_j is the Gaussian weight assigned to the j-th observation, as illustrated by the blue curve in Figure S10d. It should be noted that this is not the only possible weighting or integration strategy for deriving regional variations; other schemes may also be used, depending on the user's purpose.

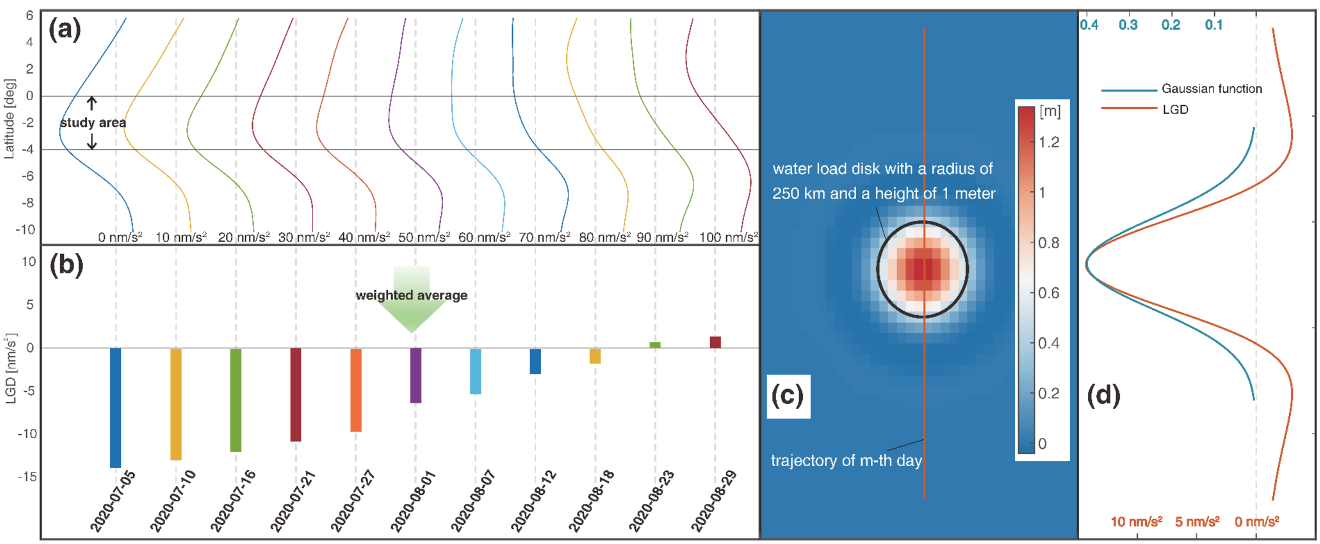

Figure S6. Gaussian-weighted construction of the regional LGD time series. (a) Along-track LGD profiles for different satellite passes. (b) Gaussian-weighted regional LGD time series. (c) Modeled LGD response and satellite ground track. (d) Gaussian weighting function and corresponding along-track weighting profile.

Section S5

The EWH is derived from the CSR RL06.3 spherical harmonic solutions. In addition to the data products, the preprocessing steps are also consistent with those used for the L2-LGD synthesis, including replacement of the degree-2 and degree-3 zonal coefficients, removal of the GOCO06s static field, and truncation to degree and order 60. In addition, decorrelation and Gaussian smoothing with a 350 km radius are applied in the spherical harmonic synthesis to derive the EWH.